BACKSCATTERING FROM PARTIALLY CONVEX TARGETS IN FREE SPACE WITH H-BEAM WAVE INCIDENCE

H. El-Ocla

Department of Computer Science
Lakehead University
955 Oliver Road, Thunder Bay, Ontario P7B 5E1, Canada

Abstract—In [9], scattering problems of plane and beam wave incidences were presented. In that study, it was found that the target configuration together with beam width have a major effect on the laser RCS (LRCS). This conclusion was proved for horizontal incident wave polarization (E-polarization) in free space. The polarization of incident waves is one of the key parameters in the scattering problems and in particular in the resonance region where the target has a comparable size with the wave length. In this work, we extend our study and investigate the impact of vertical incident wave polarization (H-polarization) on the LRCS of large size targets and compare it with RCS of targets with plane wave incidence.
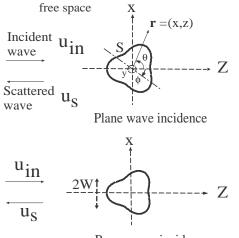
1. INTRODUCTION

Scattering problem of waves from finite size targets is of great interest for radar researchers. Different methods proposed to formulate the scattering wave were presented: examples are in [1–3] based on physical optics (PO) method, and using multiple scattering from parallel cylinders [4]. To solve the scattering problem, a method has been presented to formulate the electromagnetic waves as a boundary value problem [5]. This method is characterized by the estimation of the current on the whole surface and not only on the illumination region as in PO. Therefore this method gives an accurate calculation of the wave intensity. Drawing on this method, numerical results have been presented for RCS of conducting convex bodies such as circular and elliptic cylinders [5]. The effects of target configuration and polarization on the radar cross section (RCS) were analyzed for partially convex targets in many publications [6–9]. The effects of

plane wave incidence and target configuration together with wave polarization on the RCS were clearly explained.

To excite infinitely large plane wave fronts, an infinitely large source should be used. This cannot be available easily especially for plane waves sufficiently wide at the incidence fronts of large size targets in the far field. In an attempt to generate plane wave, an expansion of plane wave into Gaussian beam waves was derived [10]. Gaussian beams play a key role in different fields of physics; let us mention applications in lasers, electromagnetic waves, etc. Many problems of propagation and scattering of Gaussian beams have been solved (see [7, 11, 12], where other references can be found). On the other hand, the research on laser radar [13] for target ranging, detection, and recognition [14] has become the one key technology to evaluate and model the characteristics of scattering from a complex target in the military and civil applications. The scattering characteristics are analyzed through studying the behavior of laser RCS (LRCS) of the target. In doing that, one can calculate the LRCS by assuming a beam wave incident on a nonconvex target in free space. In fact, we can consider the beam wave as a plane wave when the mean size of the target becomes smaller than the beam width, however, this is not usually the general case in practice. To detect targets of larger sizes, we should, therefore, handle the case where the beam width is smaller than the target size.

Prior to this work, the characteristics of RCS with plane wave incidence and LRCS of a perfectly conducting cylinder of nonconvex cross-section for E-polarization [9] have been investigated. Polarization of incident waves is one of the key parameters in waves scattering problems. The major difference between E and H polarizations is the creeping waves produced in the latter case and in turn they circumnavigate the target when incident waves fall down on the target. The interference between direct and creeping waves usually contributes non smooth RCS behaviour in particular when target size becomes comparable with wave length in free space. A numerical study of the effect of creeping waves on LRCS of large size targets is investigated here. In doing that, the effect of the target configuration including size and curvature on LRCS of target is evaluated and compared with RCS for plane wave incidence. To achieve this aim, our method prescribed earlier is used to conduct numerical results for the RCS of concave-convex targets of large sizes up to about five wavelengths to exceed the beamwidth. Next, we estimate the normalized RCS (NRCS), defined as the ratio of LRCS σ_b to RCS σ_0 for plane wave incidence. Therefore, we will be able to analyze the difference in the behavior between σ_0 and σ_b. We consider

the two dimensional case where a directly incident wave is produced by a line source distributed uniformly along the axis parallel to the conducting cylinder (target) axis. In [6], it has been clarified that the RCS changes obviously with the illumination region curvature. In this study, we concentrate on the wave backscattering from convex illumination portion only. The time factor $\exp(-iwt)$ is assumed and suppressed in the following section.

2. FORMULATION

Consider two problems of waves scattering from targets in free space: (1) plane wave incidence, (2) beam waves incidence. For both cases, geometry of the problems is shown in Figure 1. Here, $k = \omega\sqrt{\varepsilon_0\mu_0}$ is the wavenumber in free space where ε_0 and μ_0 are the free space permittivity and magnetic permeability, respectively, and W is the beam width.

Figure 1. Geometry of the problem of wave scattering from a conducting cylinder.

Let us assume the case where a directly incident wave is produced by a line source $f(\mathbf{r}')$ distributed uniformly along the y axis. Then, the incident wave is cylindrical and becomes plane approximately around the target because the line source is very far from the target. We designate the incident wave field by $u_{in}(\mathbf{r})$, the scattered wave field by $u_s(\mathbf{r})$, and the total wave field by $u(\mathbf{r}) = u_{in}(\mathbf{r}) + u_s(\mathbf{r})$.

An electromagnetic wave radiated from the line source located at $\mathbf{r}_t$ propagates in free space, illuminates the target and induces a surface current on the target. A scattered wave from the target is produced by the surface current and propagates back to the observation point that coincides with the source point.

The target is assumed to be a conducting cylinder. The cross-section of the cylinder is expressed by

$$r = a[1 - \delta \cos 3(\theta - \phi)] \tag{1}$$

where a is the mean size of the target in which $a \ll \mathbf{r}_t$, δ is the concavity index, and ϕ is the rotation index which represents the incident angle. We deal with this scattering problem two dimensionally; therefore, we represent $\mathbf{r}$ as $\mathbf{r} = (x, z)$. Assuming an H-polarization of incident waves (H-wave incidence), we can impose the Neumann boundary condition for wave field $u(\mathbf{r})$ on the cylinder surface S. That is, $\frac{\partial}{\partial n} u(\mathbf{r}) = \mathbf{0}$, where $u(\mathbf{r})$ represents E_x. On the other hand for E-polarization of incident waves (E-wave incidence) in [9], $u(\mathbf{r})$ represented E_y assuming Dirichlet boundary condition.

Using the current generators Y_H and Green's function in free space $G_0(\mathbf{r} \mid \mathbf{r}')$, we can express the scattered wave as

$$u_\mathrm{s}(\mathbf{r}) = -\int_S d\mathbf{r}_1 \int_S d\mathbf{r}_2 \left[\left(\frac{\partial}{\partial n_2} G_0(\mathbf{r} \mid \mathbf{r}_2) \right) Y_\mathrm{H}(\mathbf{r}_2 \mid \mathbf{r}_1) u_{in}(\mathbf{r}_1 \mid \mathbf{r}_t) \right]. \tag{2}$$

For the scattering problem with plane wave incidence, $u_{in}(\mathbf{r}_1 \mid \mathbf{r}_t)$ is expressed as

$$u_{in}(\mathbf{r}_1 \mid \mathbf{r}_t) = G_0(\mathbf{r}_1 \mid \mathbf{r}_t). \tag{3}$$

Here Y_H is the operator that transforms incident waves into surface currents on S and depends only on the scattering body [5–9]. The current generator can be expressed in terms of wave functions, which satisfy Helmholtz equation and the radiation condition. That is, for H-wave incidence, the current generator is obtained as

$$Y_H(\mathbf{r} \mid \mathbf{r}') \simeq -\frac{\partial \Phi_M^*(\mathbf{r}_2)}{\partial n} A_H^{-1} \ll \Phi_M^T(\mathbf{r}') \tag{4}$$

where $\Phi_M = [\phi_{-N}, \phi_{-N+1}, \ldots, \phi_N]$, $M = 2N + 1$ is the total mode number, $\phi_m(\mathbf{r}) = H_m^{(1)}(k\rho) \exp(im\theta)$, and A_H is a positive definite

Hermitian matrix given by

$$
A_H = \begin{pmatrix} \left(\dfrac{\partial \phi_{-N}}{\partial \mathrm{n}}, \dfrac{\partial \phi_{-N}}{\partial \mathrm{n}} \right) & \cdots & \left(\dfrac{\partial \phi_{-N}}{\partial \mathrm{n}}, \dfrac{\partial \phi_{N}}{\partial \mathrm{n}} \right) \\ \vdots & \ddots & \vdots \\ \left(\dfrac{\partial \phi_{N}}{\partial \mathrm{n}}, \dfrac{\partial \phi_{-N}}{\partial \mathrm{n}} \right) & \cdots & \left(\dfrac{\partial \phi_{N}}{\partial \mathrm{n}}, \dfrac{\partial \phi_{N}}{\partial \mathrm{n}} \right) \end{pmatrix} \tag{5}
$$

in which its m, n element is the inner product of ϕ_m and ϕ_n:

$$
\left(\frac{\partial \phi_m}{\partial \mathrm{n}}, \frac{\partial \phi_n}{\partial \mathrm{n}} \right) \equiv \int_S \frac{\partial \phi_m}{\partial \mathrm{n}} \frac{\partial \phi_n^*}{\partial \mathrm{n}} \, d\mathbf{r} \tag{6}
$$

where $\ll \Phi_M^T$, denotes the operation (7) of each element of Φ_M^T and the function u_{in} to the right of Φ_M^T

$$
\ll \phi_m(\mathbf{r}), u_{in}(\mathbf{r}) \gg \equiv \phi_m(\mathbf{r}) \frac{\partial u_{in}(\mathbf{r})}{\partial n} - \frac{\partial \phi_m(\mathbf{r})}{\partial n} u_{in}(\mathbf{r}). \tag{7}
$$

The Y_H is proved to converge in the sense of mean on true operators when $M \to \infty$.

For the scattering problem with Gaussian beam wave incidence, let us consider $u_{in}(\mathbf{r}_1 \mid \mathbf{r}_t)$ to be represented by

$$
u_{in}(\mathbf{r}_1 \mid \mathbf{r}_t) = G_0(\mathbf{r}_1 \mid \mathbf{r}_t) \exp \left[- \left(\frac{kx_1}{kW} \right)^2 \right]. \tag{8}
$$

The beam expression is approximately useful only around the cylinder.

The plane wave can be considered as a beam wave with infinite beam width, that is:

$$
W = \infty \qquad \text{for plane wave incidence} \tag{9}
$$

We can obtain the RCS σ_0 for plane wave incidence using Equations (2) and (3), and obtain LRCS σ_b using Equations (2) and (8). We use σ as a general symbol that indicates both σ_0 and σ_b and can be calculated as

$$
\sigma = |u_s(\mathbf{r})|^2 \, k(4\pi z)^2. \tag{10}
$$

3. NUMERICAL RESULTS

It should be noted that N in (5) depends on the target parameters. For example, it is chosen that $N = 28$ at $\delta = 0.1$ in the range of
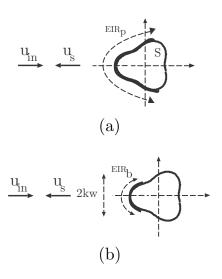
(a)

(b)

Figure 2. Geometry shows the effective illumination region where (a) plane wave incidence, (b) beam wave incidence.

$0.1 < ka < 5$; at $ka = 20$, and $N = 46$ at $\delta = 0.1$. As a result, the numerical results are accurate because these values of N lead to convergent RCS. In the numerical results, it is assumed that $\phi = \pi$.

In the numerical analysis of the RCS and LRCS, I use the terminologies of effective illumination regions EIR for plane wave EIR_p and beam wave EIR_b defined in [9] as shown in Figure 2. That is the surface illuminated by the plane wave incidence and the surface illuminated by the beam wave incidence and restricted by the $2kW$ are the definitions for EIR_p and EIR_b, respectively. Also I will refer to DRCS defined as the difference in the behavior of RCS σ with ka between plane and beam wave incidences; i.e., between σ_0 and σ_b, respectively.

For ideal target detection, σ_0 is the measurement that should be used as a reference where the target becomes fully covered by the incident waves, and consequently, DRCS should be set to tend to zero. In doing that, parameters that affect EIR including kW and ka would be chosen carefully as going to be shown in the following sections. Mean size of the target a and δ are target's parameters that have another impact on EIR and in turn on the DRCS, however, they can not obviously be controlled.

3.1. Radar Cross-section RCS

In Figures 3 and 4, I discuss the numerical results for σ_0 and σ_b. It is observed that RCS suffers from oscillated behaviour in both cases of plane and beam wave incidences. The oscillated behaviour that is absent in case of E-wave incidence is due, as a matter of fact, to the effect of creeping waves [8, 16]. At the point of tangency, each wave creeps around the surface at a velocity less than that in free space and that is attenuated by tangential radiation. For low ka values, wave can continue to creep around the target many times and, therefore, the interference between the specularly reflected and creeping waves is obvious enough to let RCS oscillates largely. However, with larger ka, the creeping waves travel along the cylinder and they become weaker and weaker the farther they have to travel due to radiation. Therefore, the creeping waves attenuation reduces its effectiveness rapidly resulting in diminishing the interference effect gradually with ka.

Also it is noticed from these figures that there are two effects on both σ_0 and σ_b. The first is the effect of target configuration and can be seen clearly with changing δ and ka as shown in Figure 3. With small ka and/or large δ, DRCS becomes small as a result of the relation $\mathrm{EIR}_p \simeq \mathrm{EIR}_b$. As ka increases and/or δ decreases, as the DRCS augments due to the lack in EIR_b, and vice versa. To understand such behavior, we have to turn the attention to the beam wave incidence case where the surface current outside EIR_b is relatively small compared to that at the beam spot that is inside the EIR_b. Therefore in accordance to (2), as EIR_b shrinks, as the contribution to the scattered waves wanes clearly. Beam width size kW is the second effect in which there is a direct relationship between σ_b and kW as shown in Figure 3. In other words, when kW increases, the results of σ_b become closer to σ_0 especially for small ka and that agrees with the conclusion published in [15]. As a result, DRCS reduces which leads to approaching accurate target detection.

In Figure 4(a), creeping waves make σ_0 oscillates largely for relatively small ka. For larger ka, σ_0 does not vary with ka because of two reasons: the effect of creeping waves reduction. Secondly, the generated surface current does not change since the illumination region is always covered by the plane wave incidence. On the other hand, in Figures 4(b), (c), σ_b lessens, in oscillated manner, as a result of the shortage in the surface current and that leads to the gradual decrease in the scattered wave contribution with ka. Also, it is observed that σ_b differs with δ for small ka and absolutely coincides with larger ka. The coincidence of σ_b becomes more obvious and earlier with ka for small kW. This occurs when $ka \gg kW$ in which the surface current outside
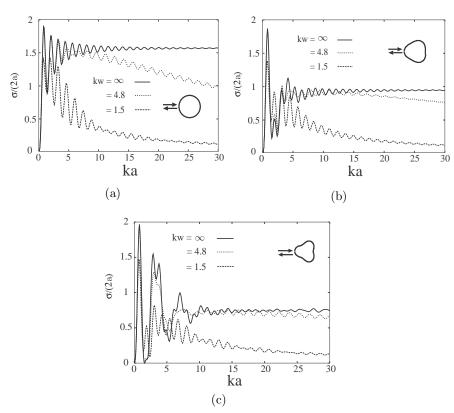
(a)

(b)

(c)

Figure 3. RCS vs. target size for H-wave incidence in free space where (a) $\delta = 0$, (b) $\delta = 0.1$, and (c) $\delta = 0.2$.

EIR_b has a slight contribution to the scattered waves with different δ. At certain limit, σ_b will diminish with large enough target and the beam wave becomes incapable of target detection. In general, σ_0 and σ_b approach with ka at certain values that are almost same as E-wave case.

3.2. Normalized RCS

NRCS, defined as the ratio of LRCS σ_b to RCS σ_0 for plane wave incidence, is considered to clarify the DRCS; numerical results for NRCS are presented in Figure 5.

NRCS is analyzed in three regions of ka compared to kW.

For $ka \ll kW$, the NRCS equals unity and this is valid independent of illumination region curvature implemented in the
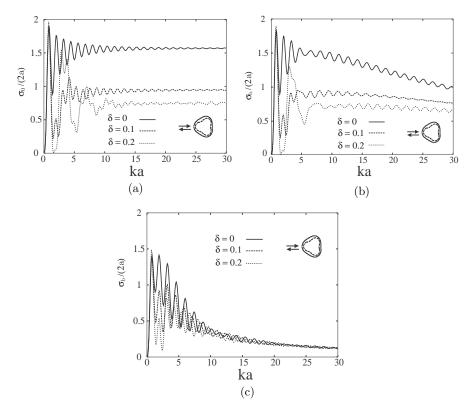
Figure 4. RCS vs. target size for different δ where (a) plane wave incidence ($kW = \infty$), (b) beam wave incidence with $kW = 4.8$, and (c) beam wave incidence with $kW = 1.5$.

concavity index δ. In this range, beam wave behaves as a plane wave for the small ka and as a result DRCS tends to zero.

For $ka \simeq kW$, NRCS oscillates largely around unity and the oscillation strength; i.e., enhancement factor, of NRCS decreases with kW while increases with δ. At certain values of target parameters ($ka = 1.6$ and $\delta = 0.2$) and in particular when $kW = 1.5$, this oscillation becomes resonant and the enhancement factor, increases dramatically and reaches a maximum as shown in Figure 5(c). This means that the enhancement occurs strongly when the target size is close to the wavelength and kW becomes quite small. This strong increase is considered as anomalous enhancement that is arised due to the creeping waves effect as explained early, a detailed study of the circumstances related to this resonance is described in [6].
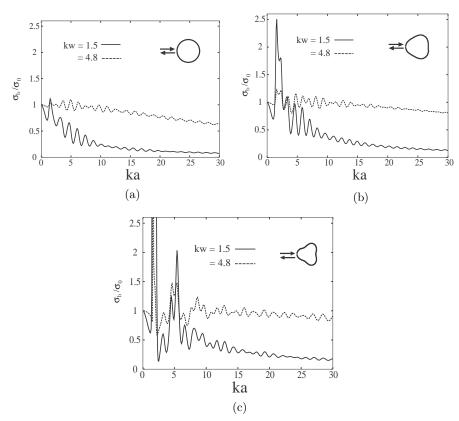
(a)

(b)

(c)

Figure 5. Normalized RCS vs. target size for H-wave incidence in free space where (a) $\delta = 0$, (b) $\delta = 0.1$, (c) $\delta = 0.2$.

For $ka > kW$, NRCS oscillates irregularly in descending amplitude with ka; this decrease is slower and NRCS is closer to one with large kW, this behavior is due to the DRCS as illustrated earlier. Also we observe that the oscillated behaviour in case of H-wave incidence is not regular sinusoidal as the case of E-wave incidence due to the effect of creeping waves. In the region $ka \gg kW$, the impact of δ becomes obviously limited on the EIR and therefore the amount of scattered waves alters slightly. Consequently, the performance of RCS seems to be similar with different δ for large ka. Compared to the results in [9], we note an interesting observation that the dwindling rate of NRCS in both cases of E-wave and H-wave incidences are quite close.

4. CONCLUSION

The effect of H-polarization of the incident wave on the behaviour of RCS of targets in free space has been analyzed numerically. We assume partially convex targets of large sizes of about five wavelengths. The scattering problems of plane wave and beam wave incidences were considered. Target configuration together with beam width kW has primary effects on laser RCS (LRCS). Creeping waves, produced in case of H-polarization, influence the LRCS obviously for limited ka and their impact diminishes gradually with ka. LRCS behaves differently from RCS for plane wave incidence in the range $ka \geq kW$ where target complexity δ has a clear effect especially with small kW. This behaviour contradicts with E-wave incidence case in which LRCS is almost invariant with δ as a result of absence of creeping waves. However, LRCS approaches certain values with $ka > kW$ irrespective of linear wave polarization.

   For accurate radar detection, beam width should be chosen wide enough around the target.

REFERENCES

1. Keller, J. B. and W. Streifer, "Complex rays with an application to Gaussian beams," *J. Opt. Soc. Am.*, Vol. 61, No. 1, 40–43, 1971.
2. Ikuno, H., "Calculation of far-scattered fields by the method of stationary phase," *IEEE Transactions on Antennas and Propagation*, Vol. AP-27, No. 2, 199–202, 1979.
3. Mieras, B. C. L., "Time domain scattering from open thin conducting surfaces," *Radio Science*, Vol. 16, No. 6, 1231–1239, 1981.
4. Elsherbeni, A. and M. Hamid, "Scattering by parallel conducting circular cylinders," *IEEE Transactions on Antennas and Propagation*, Vol. AP-35, No. 3, 355–358, 1987.
5. Meng, Z. Q. and M. Tateiba, "Radar cross sections of conducting elliptic cylinders embedded in strong continuous random media," *Waves in Random Media*, Vol. 6, 335–345, 1996.
6. El-Ocla, H. and M. Tateiba, "Strong backscattering enhancement

for partially convex targets in random media," *Waves in Random Media*, Vol. 11, No. 1, 21–32, 2001.

7. El-Ocla, H. and M. Tateiba, "An indirect estimate of RCS of conducting cylinder in random medium," *IEEE Antennas and Wireless Propagation Letters*, Vol. 2, 173–176, 2003.

8. El-Ocla, H., "Backscattering from conducting targets in continuous random media for circular polarization," *Waves in Random and Complex Media*, Vol. 15, No. 1, 91–99, 2005.

9. El-Ocla, H., "On laser radar cross section of targets with large sizes for E-polarization," *Progress in Electromagnetics Research*, PIER 56, 323–333, 2006.

10. Cerveny, V., "Expansion of a plane wave into Gaussian beams," *Studia Geophysica et Geodaetica*, Suppl. Special Issue, Vol. 46, 43–54, 2002.

11. Gardner, J. S. and R. E. Collin, "Scattering of a Gaussian laser beam by a large perfectly conducting cylinder: physical optics and exact solutions," *IEEE Transactions on Antennas and Propagation*, Vol. 52, No. 3, 642–652, 2004.

12. Sakurai, H., M. Ohki, K. Motojima, and S. Kozaki, "Scattering of Gaussian beam from a hemispherical boss on a conducting plane," *IEEE Transactions on Antennas and Propagation*, Vol. 52, No. 3, 892–894, 2004.

13. Jelalian, A. V., *Laser Radar Systems*, Artech House, Boston, Mass., 1992.

14. Steinvall, O., H. Olsson, G. Bolander, C. Carlsson, and D. Letalick, "Gated viewing for target detection and recognition," *Laser Radar Technology and Applications IV*, G. W. Kamerman and C. Werner (eds.), *Proc. SPIE*, Vol. 3707, 432–448, 1999.

15. Peng, M. Y. and W. B. Dou, "Diffraction of Gaussian beam by a periodic screen," *International Journal of Infrared and Millimeter Waves*, Vol. 22, No. 8, 1277–1286, 2001.

16. Harbold., M. L. and B. N. Steinberg, "Direct experimental verification of creeping waves," *The Journal of the Acoustical Society of America*, Vol. 45, 592–603, 1969.